Journal of Computational Applied Mechanics 2022, 53(4): 585-598

DOI: 10.22059/JCAMECH.2022.349748.763

RESEARCH PAPER

# Therapeutic Applications of Darcy-Forchheimer Hybrid Nanofluid Flow and Mass Transfer Over a Stretching Sheet

Arati Mishra [a], Kharabela Swain [b*], Suresh Dash [a]

[a] *Department of Chemistry, Siksha 'O' Anusandhan (Deemed to be University), Bhubaneswar, Odisha-751030, India*
[b] *Department of Mathematics, Gandhi Institute for Technology, Bhubaneswar-752054, India*

**Abstract**

**The purpose of the current study is to investigate the therapeutic applications of Darcy-Forchheimer flow and mass transfer of hybrid nanofluid (HNF) over a stretching sheet by the influence of magnetic field and chemical reaction. The HNF is the conglomeration of two types of nanoparticles (NPs) namely copper (metal) and alumina (metallic oxide) with water as regular fluid. Copper NPs act as an anti-biotic, anti-microbial, and anti-fungal agent whereas alumina NPs has wide range of biomedical applications including cancer therapy, biosensing, and immunotherapy etc. Thus, the present model is useful because it may be used to a variety of fields, including biomedicine, microelectronics, biology, and industrial production processes. By introducing the similarity transformations, the governing partial differential equations (PDEs) are transformed into a set of non-linear ordinary differential equations (ODEs) and then solved numerically with MATLAB bvp4c code by varying numerous operating physical parameters. It is found that higher values of magnetic, Forchheimer and slip parameters decrease the velocity profiles. Slip parameter and chemical reaction parameter has opposite effect on concentration profile. Volume fractions of NPs and slip parameter have opposite effects on skin friction coefficient and Sherwood number.**

**Keywords:** Darcy- Forchheimer flow; hybrid nanofluid; stretching sheet; magnetic field; chemical reaction.

## 1. Introduction

Hybrid nanofluid offers a wide range of applications in engineering, including the cosmetics industry, the automotive industry, the home industry, the treatment of cancer, food packaging, pharmaceuticals, fabrics, paper plastics, paints, ceramics, food colourants, and soaps due to higher thermal properties as compared to nanofluid (NF) and conventional fluid. Nanotechnology used for advanced therapy and diagnostics has significant applications in medical sciences [1]. NPs adhere to tumor cells better than normal cells, and combining impact of radiation and hypothermia is related to heat created during the repair process as a result of radiation induced DNA damage [2].

* Corresponding author. Tel.
*E-mail address: kharabela1983@gmail.com*

The primary goal of biomedical nanotechnology development is to efficiently monitor and regulate biological cell activity. Kleinstreuer et al. [3] developed biomicroelectronics mechanical systems to control the nano-drug delivery in a heated microchannel. Nowadays NFs as well as HNFs are used in cancer imaging and medication administration because of their unique characteristics of NPs. Iron-based NPs and magnetic NF are used for guiding tumors through magnet. As a consequence, cancer therapy can be improved and afflicted portions can be diagnosed without causing damage to healthy tissues. In comparison with other metal NPs, magnetic NPs are frequently utilized because they may be controlled by magnetic force. Yan and Liu [4]conducted simulation on phase change bio-heat transfer at cell levels to compare the temperatures of traditional cryosurgery with nanocryosurgery. Alghamdi et al. [5] investigate HNF MHD flow containing the medicine through blood vessels. Hassanpour et al. [6] studied the biomedical applications of aluminium oxide NPs.

The problem of flow and heat transfer caused by a stretched surface is crucial in many industrial processes, including the cooling of metallic sheets, the growth of crystals in a cooling bath, the manufacture and drawing of plastic and rubber sheets, the production of glass-fiber and paper, and metal and polymer extrusion processes. A moving surface emerges from a slit during these processes, and as a result, a boundary layer flow appears in the direction of the movement of the surface. The rate cooling has a significant impact on the quality of the final product. An advanced NF known as a HNF is one that has two different NPs dispersed in the base fluid. While this is happening, one sort of nanoparticle, first introduced by Choi and Eastman [7], is present in the common NF. Due to its capacity to increase the heat transfer rate compared to normal NF, HNF heat transfer research has gained a lot

**Nomenclature**

| | | | |
|---|---|---|---|
| $x, y$ | Cartesian coordinate system (m) | $f$ | Dimensionless velocity |
| $u, v$ | Velocity components along $x, y$ directions respectively (m/s) | $\mathrm{Re}_x$ | Local Reynolds number |
| a | constant | ***Greek symbols*** | |
| $B_0$ | Magnetic field strength | $\psi$ | Stream function |
| $C$ | Concentration | $\lambda$ | Slip parameter |
| $C_w$ | Concentration at the sheet | $\varphi$ | Dimensionless nanoparticle volume fraction |
| $C_\infty$ | Ambient concentration | $\Phi$ | Dimensionless concentration |
| $Fr$ | Forchheimer parameter | $\upsilon_{hnf}$ | Kinetic velocity of hybrid nanofluid (m$^2$/s) |
| $M$ | Magnetic parameter | $\upsilon_f$ | Kinetic velocity of base fluid (m$^2$/s) |
| $Sc$ | Schmidt number | $\sigma_{hnf}$ | Electrical conductivity of hybrid nanofluid $\left(\Omega^{-1}m^{-1}\right)$ |
| $C_b$ | Forchheimer coefficient | $\sigma_{nf}$ | Electrical conductivity of nanofluid $\left(\Omega^{-1}m^{-1}\right)$ |
| $k_c$ | chemical reaction coefficient | $\rho_{hnf}$ | Density of hybrid nanofluid (kg/m$^3$) |
| $k_r$ | chemical reaction parameter | $\rho_{nf}$ | Density of nanofluid (kg/m$^3$) |
| $D_B$ | Brownian motion coefficient (m$^2$/s) | $\rho_f$ | Density of base fluid (kg/m$^3$) |
| $C_f$ | Local skin friction coefficient | $\mu_{hnf}$ | Viscosity of hybrid nanofluid (kg/m s) |
| $Sh_x$ | Local Sherwood number | $\mu_{nf}$ | Viscosity of nanofluid (kg/m s) |

of attention in recent years. Due to this, HNF has been considered as the heat transfer fluid in the majority of heat transfer applications, including coolant in machining, electronic cooling, and transformer cooling. In particular, HNF is well known as a fluid with a higher rate of heat transmission than standard traditional fluid. Devi and Devi [8] investigated the flow of a HNF over a stretched surface while taking magnetic Cu-$Al_2O_3$ NPs into account. In their research, they found that HNF increased the rate of heat transfer more than normal NF did. The Darcy-Forchheimer flow caused by a curved stretching surface in the presence of homogeneous-heterogeneous reactions was quantitatively explored by Hayat et al. [9]. In a porous media, the Darcy-Forchheimer flow over a stretching sheet was studied by Vishnu Ganesh et al. [10] and Sahu et al. [11]. By taking into account higher-order chemical reactions and heat radiation in the presence of magnetic field, Biswas et al. [12] investigated the applicability of Maxwell NF flow across a stretching sheet. The effects of MWCNT and $Fe_3O_4$ NPs on an exponentially porous shrinking sheet with chemical reaction and slip boundary conditions were investigated by Swain et al. [13]. With a convective boundary condition, Waini et al. [14] investigated the flow of HNFs and heat transfer via a permeable stretching/shrinking surface. A HNF's stability analysis over a stretching sheet was investigated by Lund et al. [15]. Recently, Thumma et al. [16] considered that the movement of cupric oxide and silver NPs in the presence of the Coriolis force. MHD flow of a HNF across a moving plate with Joule heating was investigated by Khashi'ie et al. [17]. Various flow models have been used by numerous authors to study the flow behaviour of NFs and HNFs [18-24].

The mechanical analysis of nanostructures are investigated by using the nonlocal continuum model [25-66].

Copper has replaced silver NPs in many sectors due to lower material cost, enhanced physical as well as chemical stability and efficient mixing with polymers. Likewise, microbial mediated copper nanomaterials are gained special attention, aiming toward minimizing the overall side effects caused due to drug therapy, avoiding bioavailability, low-cost and easy to synthesize for large scale production. Due to physicochemical and structural characteristics, such as resistance to wear, chemicals, mechanical stresses, as well as their favourable optical properties and a porous vast surface area, aluminium oxide NPs have a variety of biomedical applications. Also, aluminium oxide NPs has extensive uses due to their low preparation costs and easy handling. Motivated by the above mentioned studies, the current study investigates the Darcy-Forchheimer flow and mass transfer of electromagnetic HNF over a stretched sheet considering the combination of the oxide particle alumina and the metal particle copper in the conventional fluid water. Using similarity transformation, the leading partial differential equations are converted into non-linear ordinary differential equations which are solved numerically with MATLAB bvp4c code. Graphs and tables depict the consequence of different characterizing factors on the flow model.

## 2. Mathematical Formulation of the problem

Consider a steady 2D boundary layer MHD hybrid nanofluid flow and mass transfer past a stretching sheet as shown in Fig. 1, where $x$ and $y$ are Cartesian coordinates with $x-$axis measured along the sheet and the $y-$axis normal to it. A constant magnetic field strength $B_0$ is applied in the direction of $y$-axis. The sheet is stretched with the velocity $u_w\left(x\right)=ax$ where $a>0$ is constant. The surface and ambient concentrations are $C_w$ and $C_\infty$ respectively. The magnetic Reynolds number is assumed to be small so that the induced magnetic field is neglected.

Using the above assumptions, the governing equations for steady flow of HNF following Ahmad et al. [18] are:

$$\frac{\partial u}{\partial x}+\frac{\partial u}{\partial y}=0 \tag{1}$$

$$u\frac{\partial u}{\partial x}+v\frac{\partial u}{\partial y}=\upsilon_{hnf}\frac{\partial^2 u}{\partial y^2}-\frac{\sigma_{hnf}}{\rho_{hnf}}B^2u-\frac{c_b}{\rho_{hnf}\sqrt{K}}u^2 \tag{2}$$

$$u\frac{\partial C}{\partial x}+v\frac{\partial C}{\partial y}=D_{hnf}\frac{\partial^2 C}{\partial y^2}-k_c\left(C-C_\infty\right) \tag{3}$$

The prescribed boundary conditions are

$$\left.\begin{array}{l} At\ y=0: u=u_w(x)=ax+N\dfrac{\partial u}{\partial y}, v=0, C=C_w \\ As\ y\to\infty: u\to 0, C\to C_\infty \end{array}\right\} \tag{4}$$

where $u$ and $v$ represent the velocity components of the HNF along the $x-$ axes and $y-$ axes, respectively, $C$ denotes the HNF concentration.

Further, $\mu_{hnf}, \sigma_{hnf}$, and $\rho_{hnf}$ are the dynamic viscosity, electrical conductivity, and density of the HNF, respectively. Following Gherasim et al. [67], Mintsa et al. [68], Table-1 provides the thermo physical properties of NF and HNF. In Table-1, $\varphi_1$ and $\varphi_2$ are the volume fractions of $Cu$ and $Al_2O_3$ NPs, respectively, where $\varphi_1=\varphi_2=0$ represent the regular fluid, $\mu$ represents the dynamic viscosity, $\rho$ is the density, and $\sigma$ is the electrical conductivity in which the subscripts $hnf, nf, f, n1$ and $n2$ represent HNF, NF, fluid, and solid components for $Al_2O_3$ and $Cu$ NPs, respectively. Table-2 provides the physical properties of water, $Cu$ and $Al_2O_3$ NPs [18] for a normal temperature of $298^0$K.

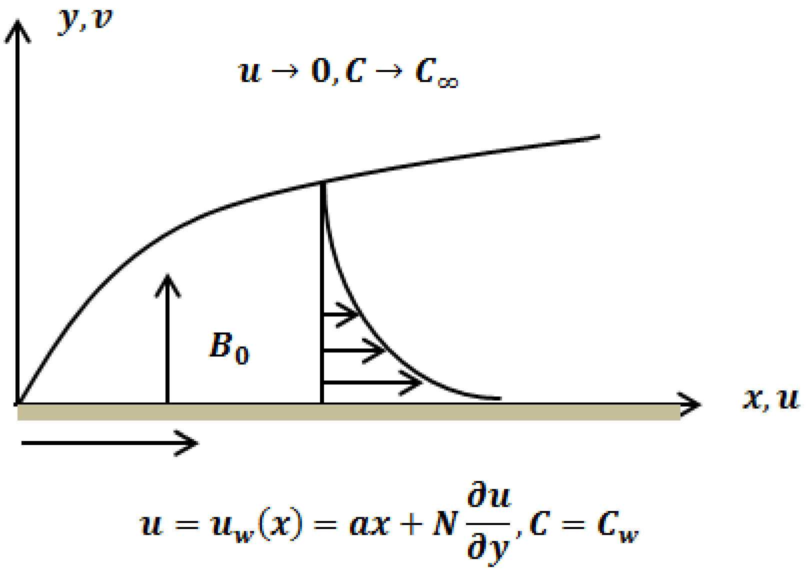


Fig. 1 Flow configuration

In order to convert the governing PDEs to non-linear ODEs, the following similarity variables are introduced.

$$u=axf'(\eta), v=-\sqrt{a\upsilon_f}\, f(\eta), C=(C_w-C_\infty)\Phi+C_\infty, \eta=y\sqrt{\frac{a}{\upsilon_f}} \tag{5}$$

where $\psi$ is the stream function defined by $u=\frac{\partial\psi}{\partial y}$ and $v=-\frac{\partial\psi}{\partial x}$ which satisfies Eq. (1).

Using Eq. (5) into Eqs. (2) and (3), we get the similarity equations as follows:

$$\frac{\mu_{hnf}/\mu_f}{\rho_{hnf}/\rho_f} f''' + ff'' - (1+Fr) f'^2 - \frac{\sigma_{hnf}/\sigma_f}{\rho_{hnf}/\rho_f} Mf' = 0 \tag{6}$$

$$(1-\varphi_1)(1-\varphi_2)\Phi'' + Sc(f\Phi' - k_r\Phi) = 0 \tag{7}$$

and the boundary conditions (4) become

$$\left.\begin{array}{l} At\,\eta=0: f(0)=0,\ f'(0)=1+\lambda f'', \Phi(0)=1, \\ As\,\eta\to\infty: f'(\eta)\to 0, \Phi(\eta)\to 0. \end{array}\right\} \tag{8}$$

where $M=\frac{\sigma_f B_0^2}{\rho_f a}$, magnetic parameter, $Fr=\frac{c_b x}{\sqrt{K}}$, Forchheimer parameter, $\lambda=N\sqrt{\frac{a}{\upsilon_f}}$, slip parameter, $k_r=\frac{k_c}{a}$, chemical reaction parameter, and $Sc=\frac{\upsilon_f}{D_B}$, Schmidt number.

The physical quantities of interest are the skin friction coefficient $C_f$ and local Sherwood number $Sh_x$ are defined as $C_f = \dfrac{2\tau_w}{\rho_{hnf} u_w^2}, Sh_x = \dfrac{x j_m}{D_{hnf}(C_w - C_\infty)}$ respectively.

Here $\tau_w$ and $j_m$ denote the shear stress and the heat flux near the surface, which are respectively given by $\tau_w = \mu_{hnf}\left(\dfrac{\partial u}{\partial y}\right)_{y=0}, j_m = -D_{hnf}\left(\dfrac{\partial C}{\partial y}\right)_{y=0}$.

Finally, we get $\mathrm{Re}_x^{1/2} C_f = \dfrac{\mu_{hnf}}{\mu_f} f''(0), \mathrm{Re}_x^{-1/2} Sh_x = -\Phi'(0)$

where $\mathrm{Re}_x = \dfrac{u_w x}{\upsilon_f}$ is the local Reynolds number.

**TABLE** 1 Thermophysical properties of NF and HNF [67, 68]

| Properties | NF | HNF |
|---|---|---|
| Density | $\rho_{nf} = (1-\varphi_1)\rho_f + \varphi_1\rho_{n1}$ | $\rho_{hnf} = (1-\varphi_2)\rho_{nf} + \varphi_2\rho_{n2}$ |
| Dynamic viscosity | $\mu_{nf} = \mu_f (0.904) e^{14.8\varphi_1}$ | $\mu_{hnf} = \mu_{nf} (0.904) e^{14.8\varphi_2}$ |
| Electrical conductivity | $\dfrac{\sigma_{nf}}{\sigma_f} = 1 + \dfrac{3\left(\dfrac{\sigma_{n1}}{\sigma_f} - 1\right)\varphi_1}{\dfrac{\sigma_{n1}}{\sigma_f} + 2 - \left(\dfrac{\sigma_{n1}}{\sigma_f} - 1\right)\varphi_1}$ | $\dfrac{\sigma_{hnf}}{\sigma_{nf}} = 1 + \dfrac{3\left(\dfrac{\sigma_{n2}}{\sigma_{nf}} - 1\right)\varphi_2}{\dfrac{\sigma_{n2}}{\sigma_{nf}} + 2 - \left(\dfrac{\sigma_{n2}}{\sigma_{nf}} - 1\right)\varphi_2}$ |

**TABLE** 2 Thermo-physical properties of water and NPs [18]

| Properties | $\rho(kg/m^3)$ | $\sigma(s/m)$ |
|---|---|---|
| water | 997.1 | $5.5\times10^{-6}$ |
| $Cu$ | 8933 | $5.96\times10^{7}$ |
| $Al_2O_3$ | 3970 | $3.69\times10^{7}$ |

**TABLE** 3 Comparison of $f''(0)$ for different values of $\lambda$ when $M = Fr = \phi_1 = \phi_2 = 0$

| $\lambda$ | $f''(0)$ | | |
|---|---|---|---|
| | Sahoo and Do [69] | Tulu and Ibrahim [70] | Present study |
| 0.0 | 1.001154 | 1.000000 | 1.002411 |
| 0.1 | 0.871447 | 0.872083 | 0.872083 |
| 0.2 | 0.774933 | 0.776377 | 0.776377 |
| 0.3 | 0.699738 | 0.701548 | 0.701548 |
| 0.5 | 0.589195 | 0.591196 | 0.591195 |
| 1.0 | 0.428450 | 0.430160 | 0.430158 |
| 2.0 | 0.282893 | 0.283981 | 0.283966 |
| 5.0 | 0.144430 | 0.144842 | 0.144798 |
| 10.0 | 0.081091 | 0.081245 | 0.081423 |
| 20.0 | 0.043748 | 0.043792 | 0.043774 |

**TABLE** 4 Computational values of $f''(0)$ and $-\Phi'(0)$ for various values of $\phi_1, \phi_2, M, Fr, \lambda, Sc$ and $k_r$

| $\phi_1$ | $\phi_2$ | $M$ | $Fr$ | $\lambda$ | $Sc$ | $k_r$ | $f''(0)$ | $-\Phi'(0)$ |
|---|---|---|---|---|---|---|---|---|
| 0 | 0 | 0.1 | 0.1 | 0.5 | 2 | 0.1 | 0.833867 | 0.943492 |
| 0.01 | | | | | | | 0.935875 | 0.957584 |
| 0.02 | | | | | | | 1.048011 | 0.972120 |
| | 0.01 | | | | | | 1.151639 | 0.990869 |
| | 0.02 | | | | | | 1.264704 | 1.009274 |
| | | 0.5 | | | | | 1.442836 | 0.977370 |
| | | 1.0 | | | | | 1.631788 | 0.944050 |
| | | | 0.5 | | | | 1.715914 | 0.933485 |
| | | | 1.0 | | | | 1.812829 | 0.921463 |
| | | | | 1.0 | | | 0.769535 | 0.739166 |
| | | | | 2.0 | | | 0.496390 | 0.653628 |
| | | | | 0 | | | 1.891098 | 0.993357 |
| | | | | 1.0 | 3 | | 0.769535 | 0.937169 |
| | | | | | 5 | | 0.769535 | 1.255357 |
| | | | | | | 0.5 | 0.769535 | 1.918332 |
| | | | | | | 1 | 0.769535 | 2.510371 |
| | | | | | | -0.5 | 0.769535 | -0.836742 |
| | | | | | | -1 | 0.769535 | -1.291888 |

## 3. Method of solution

The current study investigates the two-dimensional (2D) Darcy-Forchheimer flow and mass transfer of HNF over a stretching sheet due to the inclusion of the magnetic field and chemical reaction. The magnetized fluid in association with the NPs composed with metallic NP Copper $(Cu)$ and metallic oxide NP alumina $(Al_2O_3)$ in the base fluid water perform their characteristic. The bench mark result for the comparative study with the earlier works of Sahoo and Do [69] and Tulu and Ibrahim [60] shows a good agreement to that of the current result of shear rate in the particular case and presented in Table 3. This validates the current results as well as confirms the convergence criteria of the methodology adopted. Further, throughout the computation, we fixed the values of the non-dimensional parameters as $M = Fr = \lambda = k_r = 0.5, \phi_1 = \phi_2 = 0.01$ and $Sc = 2$ except those the particular variation is deployed in the corresponding figure.

Fig. 2 demonstrates the effect of magnetic parameter $(M)$ on the fluid velocity distribution. It is seen that velocity profiles decrease with higher values of magnetic field parameter leading to decline the velocity boundary layer thickness. Physically, the magnetic field produces a resistive force i.e. Lorentz force which opposes the motion and is responsible for reducing the fluid velocity. Further, it is observed that the velocity of HNF $(Cu - Al_2O_3 / water)$ is higher than that of NF $(Cu - water)$ and base fluid (water). Fig. 3 shows that the velocity profiles decrease with moderate values of slip parameter. As a result, the momentum boundary layer thickens as more fluid is slid over the sheet. Fig. 4 shows that velocity decreases with higher values of Forchheimer parameter. This is due to the effect inertial force that drags the fluid backward and hence the motion of fluid decreased; therefore, the velocity profile is declined. Moreover, the impacts of HNF $\left(Cu - Al_2O_3 / water\right)$ dominate when compared with the NF $\left(Cu - water\right)$.

Fig. 5 has been drawn to exhibit the impact of slip parameter on concentration distribution. It is seen that concentration profiles increase with increasing values of slip parameter in all the cases. Further, lower level of concentration is observed in case of HNF than that of NF and base fluid. Fig. 6 shows the effect of chemical reaction parameter on concentration distribution. It is seen that the increase in chemical reaction parameter decreases the concentration profiles for all the cases. It may occur due to the fact that chemical reaction helps to enhance the mass transfer and reduces the solutal boundary layer thickness. Here $k_r > 0$ relates to constructive chemical reaction. Fig. 7 shows the effect of Schmidt number $\left(Sc\right)$ on concentration distribution. Since $Sc$ is the ratio of momentum diffusivity and mass diffusivity, heavier species leads to reduce the concentration. Further, concentration for HNF, NF and base fluid are almost same in presence of chemical reaction but in absence, lower level of concentration is remarked for HNF.

Table 4 reveals that higher volume fraction of NPs favourable to increase the skin friction coefficient $\left(f''(0)\right)$ and Sherwood number $\left(-\Phi'(0)\right)$ but the opposite effect is observed in case of slip parameter. The magnetic and Forchheimer parameters are responsible to decrease $f''(0)$ and increase $-\Phi'(0)$. Further, Schmidt number and chemical reaction parameter increase the mass transfer rate at the surface so that $-\Phi'(0)$ increases.

**Flow chart**

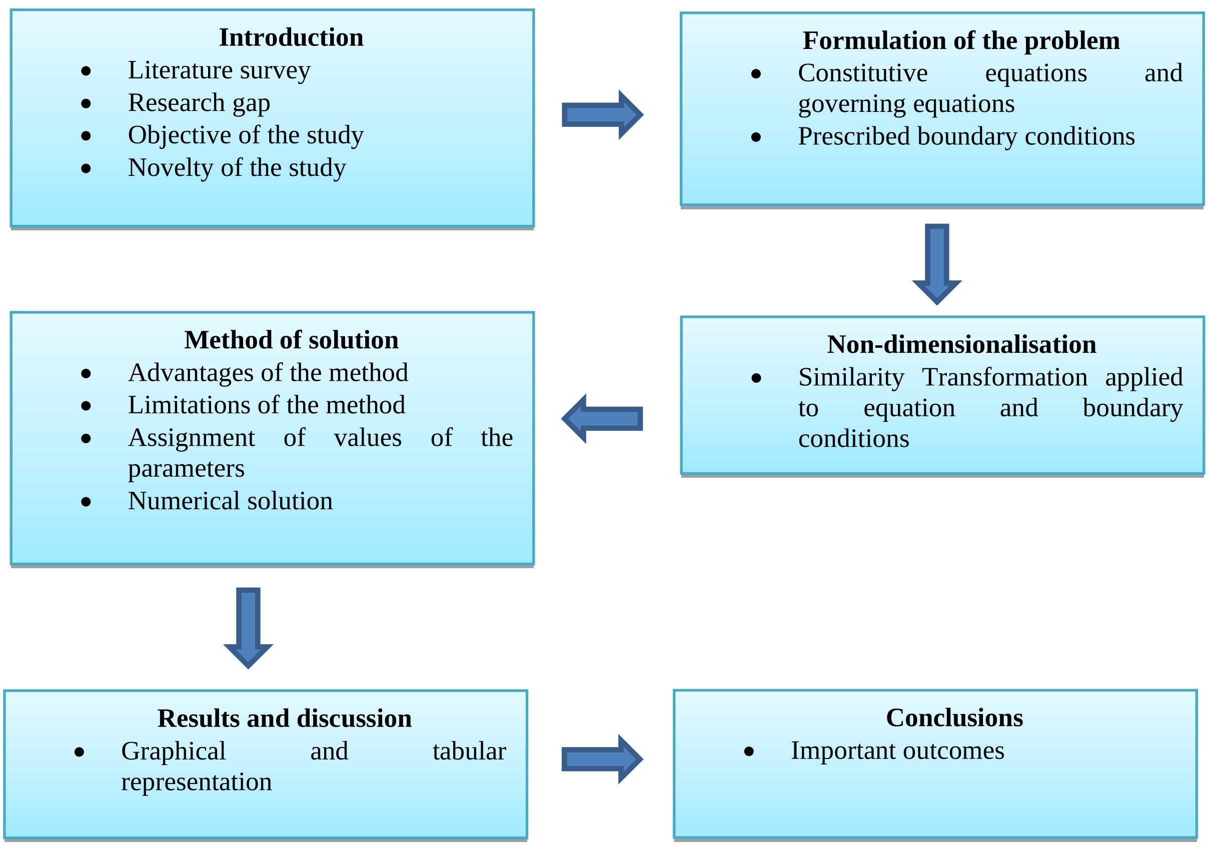


## 4. Conclusions

Numerical treatment is adopted for the Darcy-Forchheimer flow and mass transfer of hybrid nanofluid (HNF) over a stretching sheet by the influence of magnetic field and chemical reaction. The behaviour of the physical parameters is depicted through graphs and tables. Significant findings are summarized below:

- The higher values of magnetic, Forchheimer and slip parameters decrease the velocity profiles.

- Concentration profile is an increasing function of slip parameter and chemical reaction parameter.
- The presence of heavier species in the flow field (higher Sc) decreases the concentration in the boundary layer.
- Schmidt number and chemical reaction parameter boost the rate of mass transfer.
- Volume fractions of NPs and slip parameter have opposite effects on skin friction coefficient and Sherwood number.
- Volume fraction of NPs accelerates the fluid velocity whereas decelerates the concentration profile irrespective of the case of NF and the HNF that overrides the fact of the pure fluid.
- The presence of nanoparticles in the base fluid reduces the shearing stress at the plate surface so as to avoid back flow.

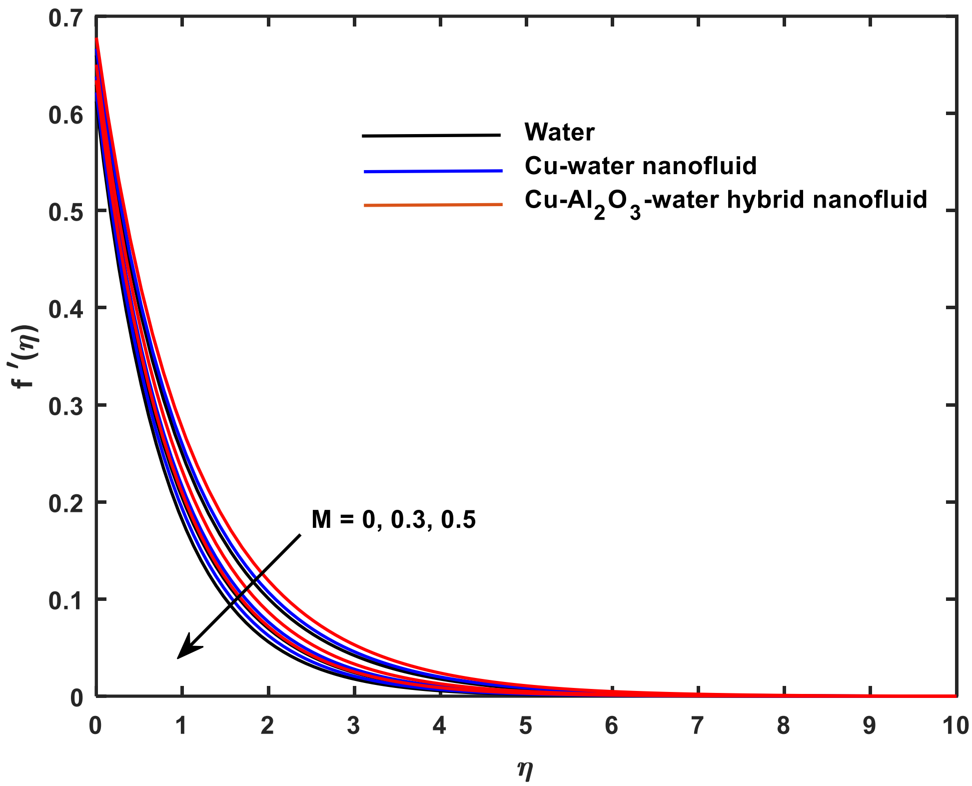


Fig. 2 Velocity distribution for various values of $M$

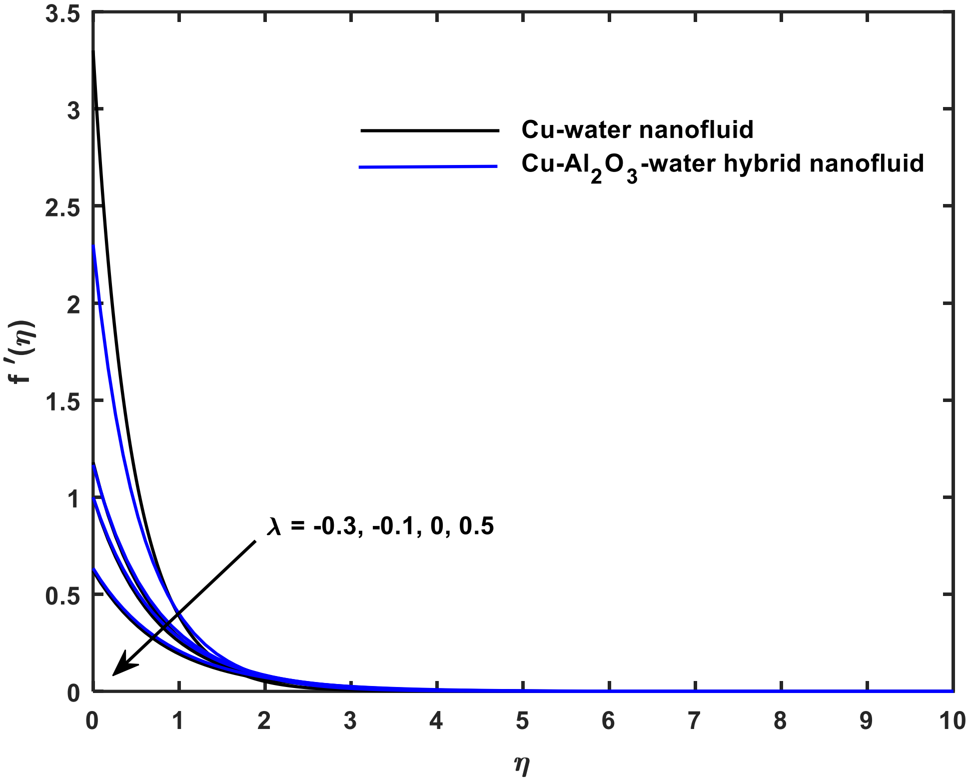


Fig. 3 Velocity distribution for various values of $\lambda$

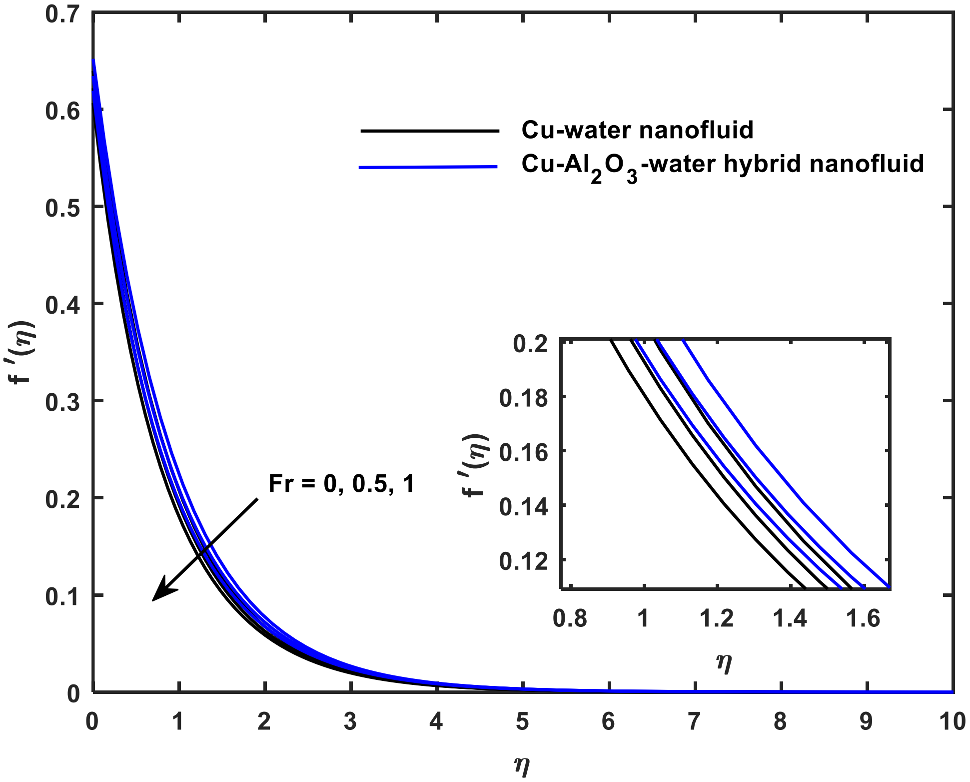


Fig. 4 Velocity distribution for various values of $Fr$

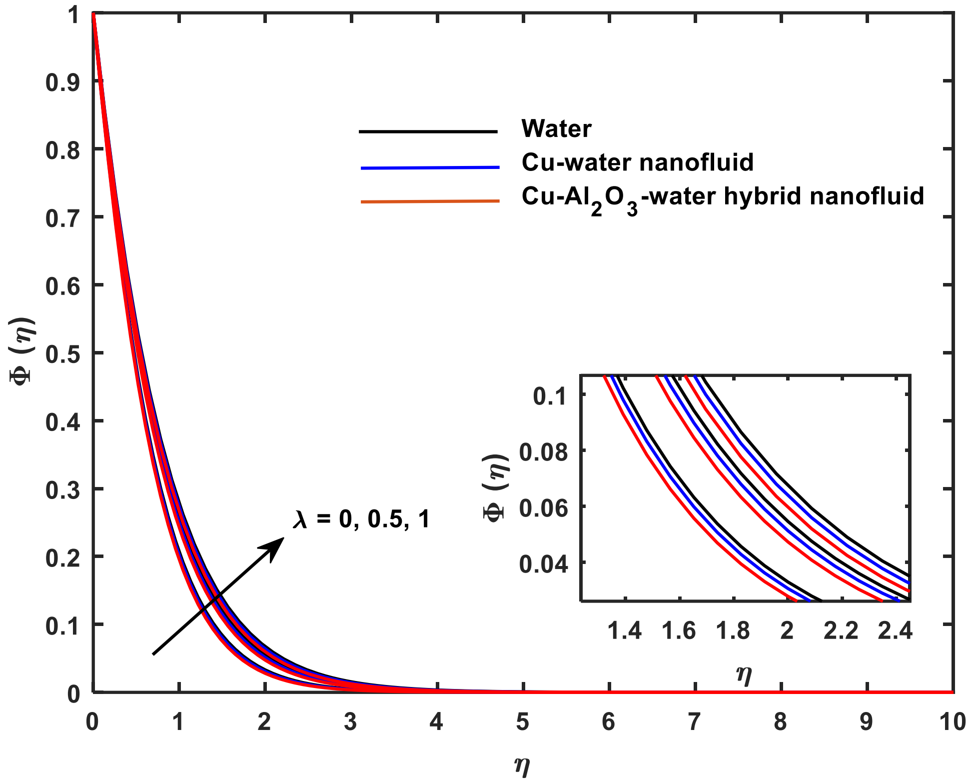


Fig. 5 Concentration distribution for various values of $\lambda$

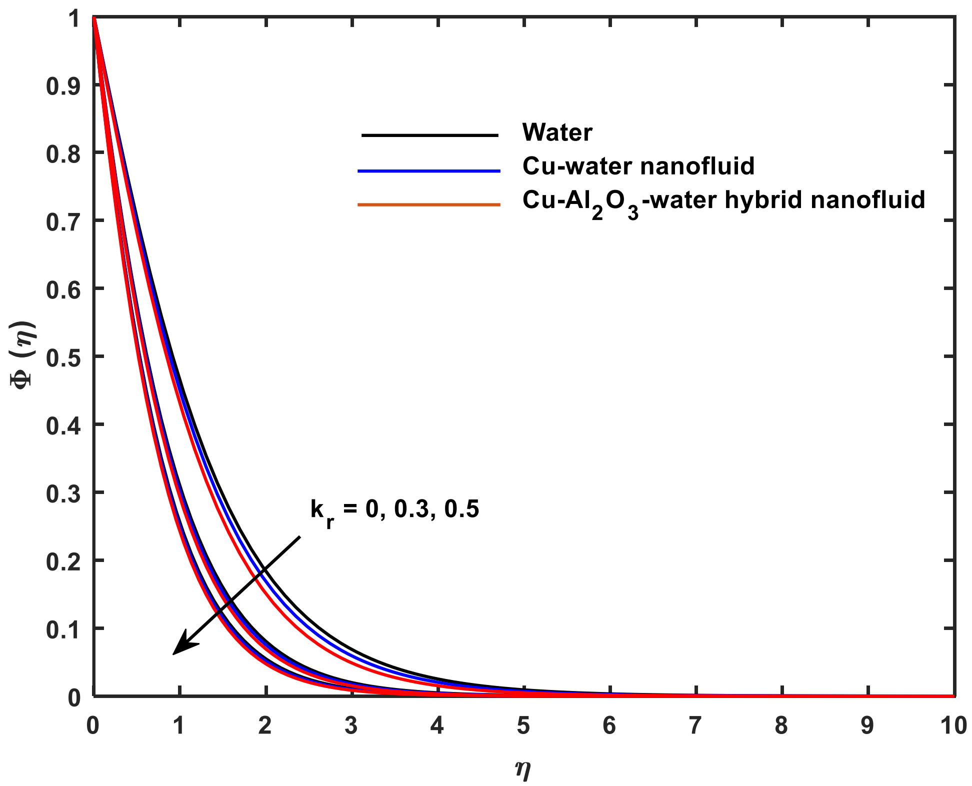


Fig. 6 Concentration distribution for various values of $k_r$

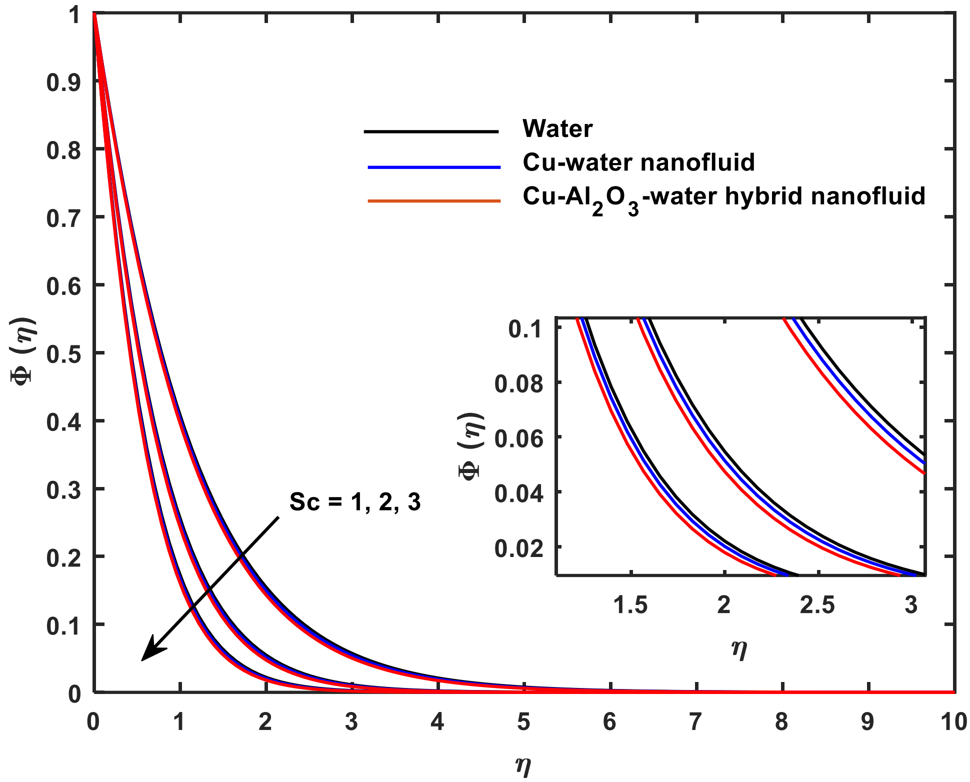


Fig. 7 Concentration distribution for various values of *Sc*

**References**


[1] B. Godin, J. H. Sakamoto, R. E. Serda, A. Grattoni, A. Bouamrani, M. Ferrari, Emerging applications of nanomedicine for the diagnosis and treatment of cardiovascular diseases, *Trends in pharmacological sciences*, Vol. 31, No. 5, pp. 199-205, 2010.

[2] V. Sridhara, B. Gowrishankar, Snehalatha, L. Satapathy, Nanofluids—a new promising fluid for cooling, *Transactions of the Indian Ceramic Society*, Vol. 68, No. 1, pp. 1-17, 2009.

[3] C. Kleinstreuer, J. Li, J. Koo, Microfluidics of nano-drug delivery, *International Journal of Heat and Mass Transfer*, Vol. 51, No. 23-24, pp. 5590-5597, 2008.

[4] J.-F. Yan, J. Liu, Nanocryosurgery and its mechanisms for enhancing freezing efficiency of tumor tissues, *Nanomedicine: Nanotechnology, Biology and Medicine*, Vol. 4, No. 1, pp. 79-87, 2008.

[5] W. Alghamdi, A. Alsubie, P. Kumam, A. Saeed, T. Gul, MHD hybrid nanofluid flow comprising the medication through a blood artery, *Scientific Reports*, Vol. 11, No. 1, pp. 1-13, 2021.

[6] P. Hassanpour, Y. Panahi, A. Ebrahimi-Kalan, A. Akbarzadeh, S. Davaran, A. N. Nasibova, R. Khalilov, T. Kavetskyy, Biomedical applications of aluminium oxide nanoparticles, *Micro & Nano Letters*, Vol. 13, No. 9, pp. 1227-1231, 2018.

[7] S. U. Choi, J. A. Eastman, *Enhancing thermal conductivity of fluids with nanoparticles*, Argonne National Lab.(ANL), Argonne, IL (United States), pp. 1995.

[8] S. A. Devi, S. S. U. Devi, Numerical investigation of hydromagnetic hybrid Cu–Al2O3/water nanofluid flow over a permeable stretching sheet with suction, *International Journal of Nonlinear Sciences and Numerical Simulation*, Vol. 17, No. 5, pp. 249-257, 2016.

[9] T. Hayat, R. S. Saif, R. Ellahi, T. Muhammad, B. Ahmad, Numerical study for Darcy-Forchheimer flow due to a curved stretching surface with Cattaneo-Christov heat flux and homogeneous-heterogeneous reactions, *Results in physics*, Vol. 7, pp. 2886-2892, 2017.

[10] N. V. Ganesh, A. A. Hakeem, B. Ganga, Darcy–Forchheimer flow of hydromagnetic nanofluid over a stretching/shrinking sheet in a thermally stratified porous medium with second order slip, viscous and Ohmic dissipations effects, *Ain Shams Engineering Journal*, Vol. 9, No. 4, pp. 939-951, 2018.

[11] S. Sahu, D. Thatoi, K. Swain, *Darcy-Forchheimer Flow Over a Stretching Sheet with Heat Source Effect: A Numerical Study*, in: *Recent Advances in Mechanical Engineering*, Eds., pp. 615-622: Springer, 2023.

[12] R. Biswas, M. S. Hossain, R. Islam, S. F. Ahmmed, S. Mishra, M. Afikuzzaman, Computational treatment of MHD Maxwell nanofluid flow across a stretching sheet considering higher-order chemical reaction and thermal radiation, *Journal of Computational Mathematics and Data Science*, Vol. 4, pp. 100048, 2022.

[13] K. Swain, F. Mebarek-Oudina, S. Abo-Dahab, Influence of MWCNT/Fe3O4 hybrid nanoparticles on an exponentially porous shrinking sheet with chemical reaction and slip boundary conditions, *Journal of Thermal Analysis and Calorimetry*, Vol. 147, No. 2, pp. 1561-1570, 2022.

[14] I. Waini, A. Ishak, I. Pop, Hybrid nanofluid flow and heat transfer past a permeable stretching/shrinking surface with a convective boundary condition, in *Proceeding of*, IOP Publishing, pp. 012022.

[15] L. A. Lund, Z. Omar, I. Khan, E.-S. M. Sherif, Dual solutions and stability analysis of a hybrid nanofluid over a stretching/shrinking sheet executing MHD flow, *Symmetry*, Vol. 12, No. 2, pp. 276, 2020.

[16] T. Thumma, N. A. Ahammad, K. Swain, I. L. Animasauan, S. Mishra, Increasing effects of Coriolis force on the cupric oxide and silver nanoparticles based nanofluid flow when thermal radiation and heat source/sink are significant, *Waves in Random and Complex Media*, pp. 1-18, 2022.

[17] N. S. Khashi'ie, N. M. Arifin, I. Pop, Magnetohydrodynamics (MHD) boundary layer flow of hybrid nanofluid over a moving plate with Joule heating, *Alexandria Engineering Journal*, Vol. 61, No. 3, pp. 1938-1945, 2022.

[18] S. Ahmad, K. Ali, M. Rizwan, M. Ashraf, Heat and mass transfer attributes of copper–aluminum oxide hybrid nanoparticles flow through a porous medium, *Case Studies in Thermal Engineering*, Vol. 25, pp. 100932, 2021.

[19] M. M. Biswal, K. Swain, G. C. Dash, K. Ojha, Study of radiative magneto-non-Newtonian fluid flow over a nonlinearly elongating sheet with Soret and Dufour effects, *Numerical Heat Transfer, Part A: Applications*, pp. 1-12, 2022.

[20] M. Basavarajappa, T. Muhammad, G. Lorenzini, K. Swain, Darcy–Forchheimer Nanoliquid Flow and Radiative Heat Transport over Convectively Heated Surface with Chemical Reaction, *Journal of Engineering Thermophysics*, Vol. 31, No. 2, pp. 261-273, 2022.

[21] M. M. Biswal, K. Swain, G. C. Dash, S. Mishra, Study of chemically reactive and thermally radiative Casson nanofluid flow past a stretching sheet with a heat source, *Heat Transfer*.

[22] K. Swain, M. Mishra, A. Kumari, Numerical study of Casson nanofluid over an elongated surface in presence of Joule heating and viscous dissipation: Buongiorno model analysis, *Journal of Computational Applied Mechanics*, Vol. 53, No. 3, pp. 414-430, 2022.

[23] W. Al-Kouz, K. Swain, B. Mahanthesh, W. Jamshed, Significance of exponential space-based heat source and inclined magnetic field on heat transfer of hybrid nanoliquid with homogeneous–heterogeneous chemical reactions, *Heat Transfer*, Vol. 50, No. 4, pp. 4086-4102, 2021.

[24] S. Mishra, R. Dalai, K. Swain, Effects of copper and titania nanoparticles on MHD 3D rotational flow over an elongating sheet with convective thermal boundary condition, *International Journal of Ambient Energy*, pp. 1-9, 2022.

[25] M. Mohammadi, A. Farajpour, A. Moradi, M. Hosseini, Vibration analysis of the rotating multilayer piezoelectric Timoshenko nanobeam, *Engineering Analysis with Boundary Elements*, Vol. 145, pp. 117-131, 2022.

[26] M. Mohammadi, A. Rastgoo, Primary and secondary resonance analysis of FG/lipid nanoplate with considering porosity distribution based on a nonlinear elastic medium, *Mechanics of Advanced Materials and Structures*, Vol. 27, No. 20, pp. 1709-1730, 2020.

[27] M. Mohammadi, M. Hosseini, M. Shishesaz, A. Hadi, A. Rastgoo, Primary and secondary resonance analysis of porous functionally graded nanobeam resting on a nonlinear foundation subjected to mechanical and electrical loads, *European Journal of Mechanics-A/Solids*, Vol. 77, pp. 103793, 2019.

[28] M. Mohammadi, A. Rastgoo, Nonlinear vibration analysis of the viscoelastic composite nanoplate with three directionally imperfect porous FG core, *Structural Engineering and Mechanics, An Int'l Journal*, Vol. 69, No. 2, pp. 131-143, 2019.

[29] A. Farajpour, A. Rastgoo, M. Mohammadi, Vibration, buckling and smart control of microtubules using piezoelectric nanoshells under electric voltage in thermal environment, *Physica B: Condensed Matter*, Vol. 509, pp. 100-114, 2017.

[30] A. Farajpour, M. H. Yazdi, A. Rastgoo, M. Loghmani, M. Mohammadi, Nonlocal nonlinear plate model for large amplitude vibration of magneto-electro-elastic nanoplates, *Composite Structures*, Vol. 140, pp. 323-336, 2016.

[31] A. Farajpour, M. Yazdi, A. Rastgoo, M. Mohammadi, A higher-order nonlocal strain gradient plate model for buckling of orthotropic nanoplates in thermal environment, *Acta Mechanica*, Vol. 227, No. 7, pp. 1849-1867, 2016.

[32] M. Mohammadi, M. Safarabadi, A. Rastgoo, A. Farajpour, Hygro-mechanical vibration analysis of a rotating viscoelastic nanobeam embedded in a visco-Pasternak elastic medium and in a nonlinear thermal environment, *Acta Mechanica*, Vol. 227, No. 8, pp. 2207-2232, 2016.

[33] M. R. Farajpour, A. Rastgoo, A. Farajpour, M. Mohammadi, Vibration of piezoelectric nanofilm-based electromechanical sensors via higher-order non-local strain gradient theory, *Micro & Nano Letters*, Vol. 11, No. 6, pp. 302-307, 2016.

[34] M. Baghani, M. Mohammadi, A. Farajpour, Dynamic and stability analysis of the rotating nanobeam in a nonuniform magnetic field considering the surface energy, *International Journal of Applied Mechanics*, Vol. 8, No. 04, pp. 1650048, 2016.

[35] M. Goodarzi, M. Mohammadi, M. Khooran, F. Saadi, Thermo-mechanical vibration analysis of FG circular and annular nanoplate based on the visco-pasternak foundation, *Journal of Solid Mechanics*, Vol. 8, No. 4, pp. 788-805, 2016.

[36] H. Asemi, S. Asemi, A. Farajpour, M. Mohammadi, Nanoscale mass detection based on vibrating piezoelectric ultrathin films under thermo-electro-mechanical loads, *Physica E: Low-dimensional Systems and Nanostructures*, Vol. 68, pp. 112-122, 2015.

[37] M. Safarabadi, M. Mohammadi, A. Farajpour, M. Goodarzi, Effect of surface energy on the vibration analysis of rotating nanobeam, 2015.

[38] M. Goodarzi, M. Mohammadi, A. Gharib, Techno-Economic Analysis of Solar Energy for Cathodic Protection of Oil and Gas Buried Pipelines in Southwestern of Iran, in *Proceeding of*, https://publications.waset.org/abstracts/33008/techno-economic-analysis-of …, pp.

[39] M. Mohammadi, A. A. Nekounam, M. Amiri, The vibration analysis of the composite natural gas pipelines in the nonlinear thermal and humidity environment, in *Proceeding of*, https://civilica.com/doc/540946/, pp.

[40] M. Goodarzi, M. Mohammadi, M. Rezaee, Technical Feasibility Analysis of PV Water Pumping System in Khuzestan Province-Iran, in *Proceeding of*, https://publications.waset.org/abstracts/18930/technical-feasibility …, pp.

[41] M. Mohammadi, A. Farajpour, A. Moradi, M. Ghayour, Shear buckling of orthotropic rectangular graphene sheet embedded in an elastic medium in thermal environment, *Composites Part B: Engineering*, Vol. 56, pp. 629-637, 2014.

[42] M. Mohammadi, A. Moradi, M. Ghayour, A. Farajpour, Exact solution for thermo-mechanical vibration of orthotropic mono-layer graphene sheet embedded in an elastic medium, *Latin American Journal of Solids and Structures*, Vol. 11, pp. 437-458, 2014.

[43] M. Mohammadi, A. Farajpour, M. Goodarzi, F. Dinari, Thermo-mechanical vibration analysis of annular and circular graphene sheet embedded in an elastic medium, *Latin American Journal of Solids and Structures*, Vol. 11, pp. 659-682, 2014.

[44] M. Mohammadi, A. Farajpour, M. Goodarzi, Numerical study of the effect of shear in-plane load on the vibration analysis of graphene sheet embedded in an elastic medium, *Computational Materials Science*, Vol. 82, pp. 510-520, 2014.

[45] A. Farajpour, A. Rastgoo, M. Mohammadi, Surface effects on the mechanical characteristics of microtubule networks in living cells, *Mechanics Research Communications*, Vol. 57, pp. 18-26, 2014.

[46] S. R. Asemi, M. Mohammadi, A. Farajpour, A study on the nonlinear stability of orthotropic single-layered graphene sheet based on nonlocal elasticity theory, *Latin American Journal of Solids and Structures*, Vol. 11, pp. 1541-1546, 2014.

[47] M. Goodarzi, M. Mohammadi, A. Farajpour, M. Khooran, Investigation of the effect of pre-stressed on vibration frequency of rectangular nanoplate based on a visco-Pasternak foundation, 2014.

[48] S. Asemi, A. Farajpour, H. Asemi, M. Mohammadi, Influence of initial stress on the vibration of double-piezoelectric-nanoplate systems with various boundary conditions using DQM, *Physica E: Low-dimensional Systems and Nanostructures*, Vol. 63, pp. 169-179, 2014.

[49] S. Asemi, A. Farajpour, M. Mohammadi, Nonlinear vibration analysis of piezoelectric nanoelectromechanical resonators based on nonlocal elasticity theory, *Composite Structures*, Vol. 116, pp. 703-712, 2014.

[50] M. Mohammadi, M. Ghayour, A. Farajpour, Free transverse vibration analysis of circular and annular graphene sheets with various boundary conditions using the nonlocal continuum plate model, *Composites Part B: Engineering*, Vol. 45, No. 1, pp. 32-42, 2013.

[51] M. Mohammadi, M. Goodarzi, M. Ghayour, A. Farajpour, Influence of in-plane pre-load on the vibration frequency of circular graphene sheet via nonlocal continuum theory, *Composites Part B: Engineering*, Vol. 51, pp. 121-129, 2013.

[52] M. Mohammadi, A. Farajpour, M. Goodarzi, R. Heydarshenas, Levy type solution for nonlocal thermo-mechanical vibration of orthotropic mono-layer graphene sheet embedded in an elastic medium, *Journal of Solid Mechanics*, Vol. 5, No. 2, pp. 116-132, 2013.

[53] M. Mohammadi, A. Farajpour, M. Goodarzi, H. Mohammadi, Temperature Effect on Vibration Analysis of Annular Graphene Sheet Embedded on Visco-Pasternak Foundati, *Journal of Solid Mechanics*, Vol. 5, No. 3, pp. 305-323, 2013.

[54] M. Danesh, A. Farajpour, M. Mohammadi, Axial vibration analysis of a tapered nanorod based on nonlocal elasticity theory and differential quadrature method, *Mechanics Research Communications*, Vol. 39, No. 1, pp. 23-27, 2012.

[55] A. Farajpour, A. Shahidi, M. Mohammadi, M. Mahzoon, Buckling of orthotropic micro/nanoscale plates under linearly varying in-plane load via nonlocal continuum mechanics, *Composite Structures*, Vol. 94, No. 5, pp. 1605-1615, 2012.

[56] M. Mohammadi, M. Goodarzi, M. Ghayour, S. Alivand, Small scale effect on the vibration of orthotropic plates embedded in an elastic medium and under biaxial in-plane pre-load via nonlocal elasticity theory, 2012.

[57] A. Farajpour, M. Mohammadi, A. Shahidi, M. Mahzoon, Axisymmetric buckling of the circular graphene sheets with the nonlocal continuum plate model, *Physica E: Low-dimensional Systems and Nanostructures*, Vol. 43, No. 10, pp. 1820-1825, 2011.

[58] A. Farajpour, M. Danesh, M. Mohammadi, Buckling analysis of variable thickness nanoplates using nonlocal continuum mechanics, *Physica E: Low-dimensional Systems and Nanostructures*, Vol. 44, No. 3, pp. 719-727, 2011.

[59] H. Moosavi, M. Mohammadi, A. Farajpour, S. Shahidi, Vibration analysis of nanorings using nonlocal continuum mechanics and shear deformable ring theory, *Physica E: Low-dimensional Systems and Nanostructures*, Vol. 44, No. 1, pp. 135-140, 2011.

[60] M. Mohammadi, M. Ghayour, A. Farajpour, Analysis of free vibration sector plate based on elastic medium by using new version differential quadrature method, *Journal of solid mechanics in engineering*, Vol. 3, No. 2, pp. 47-56, 2011.

[61] A. Farajpour, M. Mohammadi, M. Ghayour, Shear buckling of rectangular nanoplates embedded in elastic medium based on nonlocal elasticity theory, in *Proceeding of*, www.civilica.com/Paper-ISME19-ISME19_390.html, pp. 390.

[62] M. Mohammadi, A. Farajpour, A. R. Shahidi, Higher order shear deformation theory for the buckling of orthotropic rectangular nanoplates using nonlocal elasticity, in *Proceeding of*, www.civilica.com/Paper-ISME19-ISME19_391.html, pp. 391.

[63] M. Mohammadi, A. Farajpour, A. R. Shahidi, Effects of boundary conditions on the buckling of single-layered graphene sheets based on nonlocal elasticity, in *Proceeding of*, www.civilica.com/Paper-ISME19-ISME19_382.html, pp. 382.

[64] M. Mohammadi, M. Ghayour, A. Farajpour, Using of new version integral differential method to analysis of free vibration orthotropic sector plate based on elastic medium, in *Proceeding of*, www.civilica.com/Paper-ISME19-ISME19_497.html, pp. 497.

[65] N. Ghayour, A. Sedaghat, M. Mohammadi, Wave propagation approach to fluid filled submerged visco-elastic finite cylindrical shells, 2011.

[66] M. Mohammadi, A. Farajpour, A. Rastgoo, Coriolis effects on the thermo-mechanical vibration analysis of the rotating multilayer piezoelectric nanobeam, *Acta Mechanica*, https://doi.org/10.1007/s00707-022-03430-0, 2023.

[67] I. Gherasim, G. Roy, C. T. Nguyen, D. Vo-Ngoc, Experimental investigation of nanofluids in confined laminar radial flows, *International Journal of Thermal Sciences*, Vol. 48, No. 8, pp. 1486-1493, 2009.

[68] H. A. Mintsa, G. Roy, C. T. Nguyen, D. Doucet, New temperature dependent thermal conductivity data for water-based nanofluids, *International journal of thermal sciences*, Vol. 48, No. 2, pp. 363-371, 2009.

[69] B. Sahoo, Y. Do, Effects of slip on sheet-driven flow and heat transfer of a third grade fluid past a stretching sheet, *International Communications in Heat and Mass Transfer*, Vol. 37, No. 8, pp. 1064-1071, 2010.

[70] A. Tulu, W. Ibrahim, Effects of second-order slip flow and variable viscosity on natural convection flow of/water hybrid nanofluids due to stretching surface, *Mathematical Problems in Engineering*, Vol. 2021, 2021.